

# Determination of Vanadium Solubility in the Al<sub>2</sub>O<sub>3</sub>-CaO(30 Mass Pct)-SiO<sub>2</sub> and Al<sub>2</sub>O<sub>3</sub>-CaO(35 Mass Pct)-SiO<sub>2</sub> System

MIKAEL LINDVALL and DU SICHEN

The solubility of vanadium oxide in the Al<sub>2</sub>O<sub>3</sub>-CaO(30 mass pct)-SiO<sub>2</sub> system and Al<sub>2</sub>O<sub>3</sub>-CaO(35 mass pct)-SiO<sub>2</sub> system was determined experimentally at 1873 K (1600 °C) and at a fixed oxygen potential of  $9.37 \times 10^{-11}$  bar. EPMA microanalyses were employed to identify the phases and their compositions in the quenched samples. The solubility of vanadium oxide in the liquid phase was found to decrease with increasing CaO content in the liquid. The vanadium oxide solubility was especially low when both CaO and Al<sub>2</sub>O<sub>3</sub> contents were high in the liquid phase. The maximum solubility of vanadium oxide was up to 7 mass pct (as V). Two solid phases were found, a solid solution of Al<sub>2</sub>O<sub>3</sub> and vanadium oxide and an Al<sub>2</sub>O<sub>3</sub>-rich solid phase with 16.7 mass pct V<sub>2</sub>O<sub>3</sub>. The Al<sub>2</sub>O<sub>3</sub> solubility in the solid solution was found to increase with increasing Al<sub>2</sub>O<sub>3</sub> content in the liquid, the impact of the CaO content in the liquid on the solubility of Al<sub>2</sub>O<sub>3</sub> in V<sub>2</sub>O<sub>3</sub> was found to be small. The Al<sub>2</sub>O<sub>3</sub>-rich solid phase was identified as the mineral hibonite with fractionation of V into the crystal structure.

DOI: 10.1007/s11663-014-0237-2

© The Minerals, Metals & Materials Society and ASM International 2014

## I. INTRODUCTION

ACCORDING to environmental legislation in some countries, *e.g.*, Sweden, external use of steel slag from ore-based steelmaking is restricted primarily due to its content of vanadium (V) and chromium (Cr). The aggregated amount of V in discharged steel slag in the Nordic countries is yearly close to 8000 tons. Earlier work has investigated the possibility to extract V into a slag phase by bubbling carbon dioxide (CO<sub>2</sub>) into a V-alloy produced by reduction of V-bearing steel slags.<sup>[1]</sup> An initial slag having the composition of 40 mass pct (percent) Al<sub>2</sub>O<sub>3</sub>, 25 pct CaO, and 35 pct SiO<sub>2</sub> was found suitable to enhance the oxidation of V and limit the oxidation of iron (Fe) and phosphorus (P) in the oxygen partial pressure range between  $1.46 \times 10^{-11}$  and  $1.31 \times 10^{-10}$  bar.<sup>[1,2]</sup> The V-solubility in liquid in the Al<sub>2</sub>O<sub>3</sub>-CaO(25 pct)-SiO<sub>2</sub> system was determined experimentally to be maximum up to 7 mass pct (as V) at 1873 K (1600 °C) and at a fixed oxygen potential of  $9.37 \times 10^{-11}$  bar.<sup>[1]</sup> Samples above the saturation point were found to be in a 2-phase equilibrium region consisting of a liquid phase and a solid solution of aluminum oxide (Al<sub>2</sub>O<sub>3</sub>) and vanadium oxide (VA phase).<sup>[1]</sup> The existence of the VA phase resulted in high viscosity of the slag.<sup>[1,2]</sup> Since the fluidity of the slag is very important for the development of the process of vanadium extraction, the phase diagram information is essential for the design of process for vanadium extraction.

The present work aims at an experimental determination of the V-solubilities in slags. It focuses on the V-solubility in Al<sub>2</sub>O<sub>3</sub>-CaO(30 pct)-SiO<sub>2</sub> and Al<sub>2</sub>O<sub>3</sub>-CaO(35 pct)-SiO<sub>2</sub> system at 1873 K (1600 °C) and at a fixed oxygen potential of  $9.37 \times 10^{-11}$  bar.

## II. EXPERIMENTAL SETUP AND PROCEDURE

A detailed description of the equipment and the experimental procedure can be found in a previous publication.<sup>[1]</sup> Only a salient feature of the setup is given here to orientate the readers. Al<sub>2</sub>O<sub>3</sub>, CaO, and SiO<sub>2</sub> powders were dried at 1273 K (1000 °C) for 24 hours to remove moisture and CO<sub>2</sub>. The V<sub>2</sub>O<sub>5</sub> powder was dried at 373 K (100 °C) for 24 hours. The suppliers and purities of the powders are listed in Table I. Samples were then prepared by mixing appropriate ratios of the dried oxide powders in an agate mortar. The ratios of the mixed powders for all samples are shown in Table II. Each sample weighed about 1 g. Either Platinum (Pt) or Molybdenum (Mo) crucibles were used to hold the samples. Pt-crucibles were made from a tube (OD: 10 mm) with thin wall by pressing the bottom together and folding the pressed part twice. The height of the Pt-crucibles was about 25 mm. Mo-crucibles with a dimension of OD: 10 mm, ID: 8 mm, and H: 25 mm were primary used, as platinum was found to dissolve in slags with high SiO<sub>2</sub> content. The oxide powder was packed into the crucibles with the aid of a small Fe-rod. Pt-crucibles were first placed inside high density alumina crucible to prevent contact between platinum and the sample holder made of molybdenum.

The experimental setup is presented in Figure 1. A vertical resistance furnace with MoSi<sub>2</sub> heating elements

MIKAEL LINDVALL, Researcher, is with the Metallurgical and Environmental Department, Swerea MEFOS AB, Box 812, 971 25 Luleå, Sweden. DU SICHEN, Professor, is with the Department of Materials Science and Engineering, KTH Royal Institute of Technology, 100 44 Stockholm, Sweden. Contact e-mail: sichen@kth.se

Manuscript submitted October 16, 2014.

Article published online November 6, 2014.

**Table I. The Chemicals Along with Their Suppliers and Purities**

Powder	Supplier	Purity (Mass Pct)
Al <sub>2</sub> O <sub>3</sub>	Alfa Aesar	99.5
CaO	Alfa Aesar	99.95
SiO <sub>2</sub>	Roth	>99
V <sub>2</sub> O <sub>5</sub>	Alfa Aesar	99.99

and Al<sub>2</sub>O<sub>3</sub> working tube (OD: 69.9 mm, ID: 63.5 mm, H: 1000 mm) was used. In order to quench the sample rapidly, the alumina reaction tube was interconnected to a water-cooled brass tube. This arrangement allowed the sample being quenched without withdrawal from the furnace. A molybdenum sample holder was connected to a double-walled water-cooled stainless steel tube. The stainless

**Table II. The Weighed Composition of the Samples**

Sample ID	Comp. (Mass Pct)				Cruc. Mat.
	Al <sub>2</sub> O <sub>3</sub>	CaO	SiO <sub>2</sub>	V <sub>2</sub> O <sub>5</sub>	
1	3.92	22.52	61.67	11.89	Pt
2	7.67	23.02	46.04	23.27	Mo
3	44.24	23.60	22.61	9.54	Mo
4	9.69	28.10	44.57	17.64	Mo
5	24.48	28.39	35.25	11.88	Mo
6	19.58	28.39	40.14	11.88	Mo
7	14.69	28.39	45.04	11.88	Mo
8	9.79	28.39	49.93	11.88	Mo
9	4.90	28.39	54.83	11.88	Mo
10	33.29	28.39	26.44	11.88	Mo
11	24.22	28.10	30.04	17.64	Mo
12	14.53	28.10	39.73	17.64	Mo
13	9.69	28.10	44.57	17.64	Mo
14	4.84	28.10	49.42	17.64	Mo
15	19.66	28.51	42.28	9.54	Mo
16	1.97	33.57	57.27	7.19	Mo

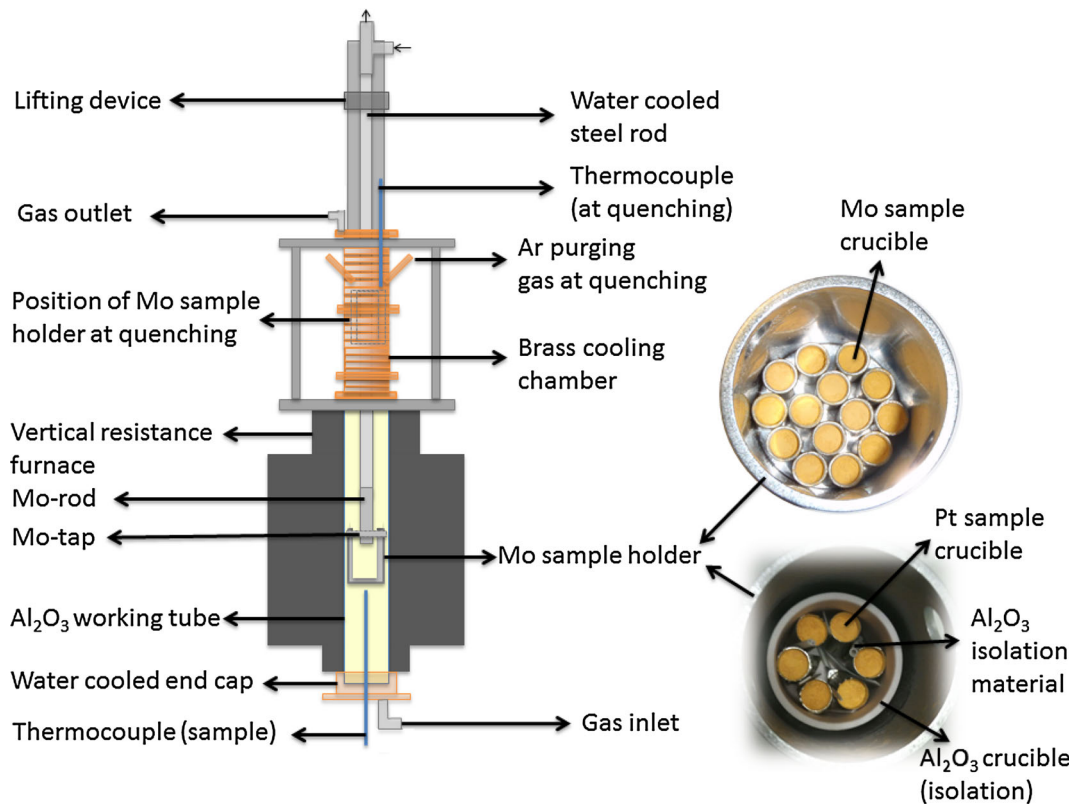


Fig. 1—Schematic presentation of the experimental setup.

steel tube was connected to a lifting unit. A B-type thermocouple was placed <10 mm below the sample holder for temperature measurement.

The samples were then lowered down using the lifting system to the even temperature zone of the reaction chamber. The reaction chamber was sealed by the use of O-rings. The system was evacuated with a vacuum pump and thereafter filled with high-purity argon. This procedure was repeated at least 3 times. After the last evacuation, the chamber was filled with a pre-mixed CO–CO<sub>2</sub>(2.3 vol. pct) gas mixture. The oxygen partial pressure for this gas mixture was calculated to be  $9.37 \times 10^{-11}$  bar with an uncertainty of  $\pm 3.8 \times 10^{-12}$  at 1873 K (1600 °C).<sup>[1]</sup> Throughout the heating and equilibration period, the CO–CO<sub>2</sub> gas mixture was flushed through the chamber.

The samples were heated up at a rate of 2 K/min. After reaching 1873 K (1600 °C), the sample was kept in the furnace for 48 hours before quenching. A flow of CO–CO<sub>2</sub> gas mixture was maintained at a flow rate of about 0.1 L/min at standard ambient temperature [298 K (25 °C)] and pressure (1 bar) (hereinafter referred to as NL/min) throughout the whole equilibrating period. Argon gas was flushed into the cooling chamber to enhance the quenching, with a flow rate of 5 NL/min. A thermocouple of type S was positioned about 10 mm above the sample holder in the quenching chamber. The thermocouples showed that the sample temperature was brought down below 1000 K (727 °C) very fast, which was far below the solidus temperature.

Electron probe microanalysis was carried out on the cross-section of each sample to gain accurate quantitative information of the phases. For this purpose, a Jeol JXA-8100 microprobe equipped with four Wavelength-Dispersive Spectrometer (WDS) was employed.

### III. RESULTS

The reliability of the present experimental technique is presented in a previous work.<sup>[1]</sup> Totally 11 samples were investigated for the Al<sub>2</sub>O<sub>3</sub>-CaO(30 pct)-SiO<sub>2</sub>-VO<sub>x</sub> system and totally five samples for the Al<sub>2</sub>O<sub>3</sub>-CaO(35 pct)-SiO<sub>2</sub>-VO<sub>x</sub> system. All samples were equilibrated at 1873 K (1600 °C) and at an oxygen potential of  $9.37 \times 10^{-11}$  bar.

Totally three phases are identified in the samples, namely (1) liquid phase, (2) a solid solution of Al<sub>2</sub>O<sub>3</sub> and vanadium oxide named as VA, and (3) an Al<sub>2</sub>O<sub>3</sub>-rich solid phase with 16.7 mass pct V<sub>2</sub>O<sub>3</sub> named as CAV. It is well known that the fractions of vanadium cations vary with the oxygen potential. V<sup>3+</sup> and V<sup>4+</sup> would be dominant at low oxygen partial pressure and low basicity in metallurgical slags. In order to present the result, V<sub>2</sub>O<sub>3</sub> is used to describe the compositions of both liquid and solid phase.

The samples consisted either of only a liquid phase (L) or a 2-phase equilibrium of L and the solid VA phase or a 3-phase equilibrium of L, solid VA phase, and solid CAV phase.

As an example, Figure 2 presents the SEM microphotograph for a sample with only liquid phase; Figure 3 presents the SEM microphotograph of the 2-phase equilibrium of L and VA; and Figure 4 presents the SEM microphotograph of the 3-phase equilibrium of L, VA, and CAV.

The phases found in the Al<sub>2</sub>O<sub>3</sub>-CaO-SiO<sub>2</sub>-V<sub>2</sub>O<sub>3</sub> system as well as the average compositions (over six measured values) of the liquid phase are presented in Table III. In the table, L stands for the liquid phase, and VA and CAV for the solid phases. V<sub>2</sub>O<sub>3</sub> is used to describe the compositions of both liquid and solid phase. Note that the compositions are normalized values. Normalization was done by taking the sum of the four components as 100 pct.

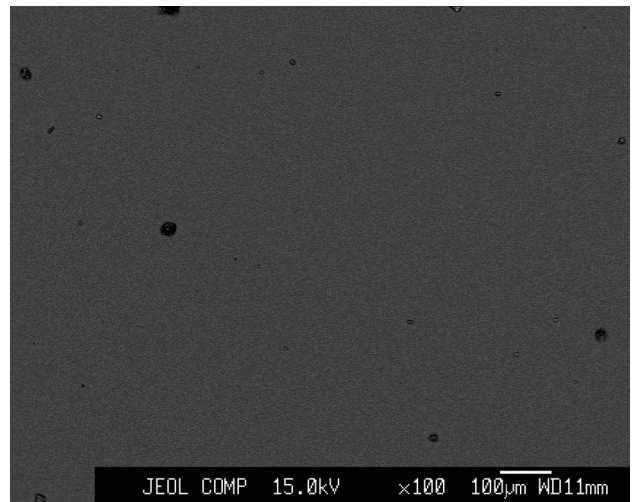


Fig. 2—Microphotograph of sample no. 1 consisting of 1-phase, *i.e.*, the liquid (L) phase.

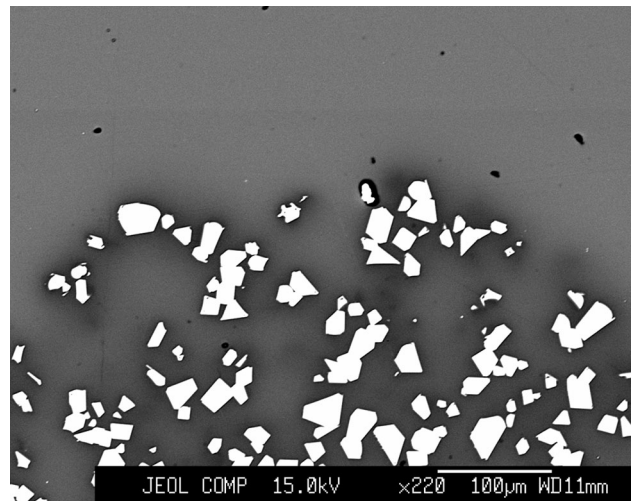


Fig. 3—Microphotograph of sample no. 7 showing the 2-phase equilibrium of the liquid—(L) and the solid V<sub>2</sub>O<sub>3</sub>-Al<sub>2</sub>O<sub>3</sub> phase (VA). The supercooled continuous liquid phase (L) is dark gray and the solid VA phase is light gray.



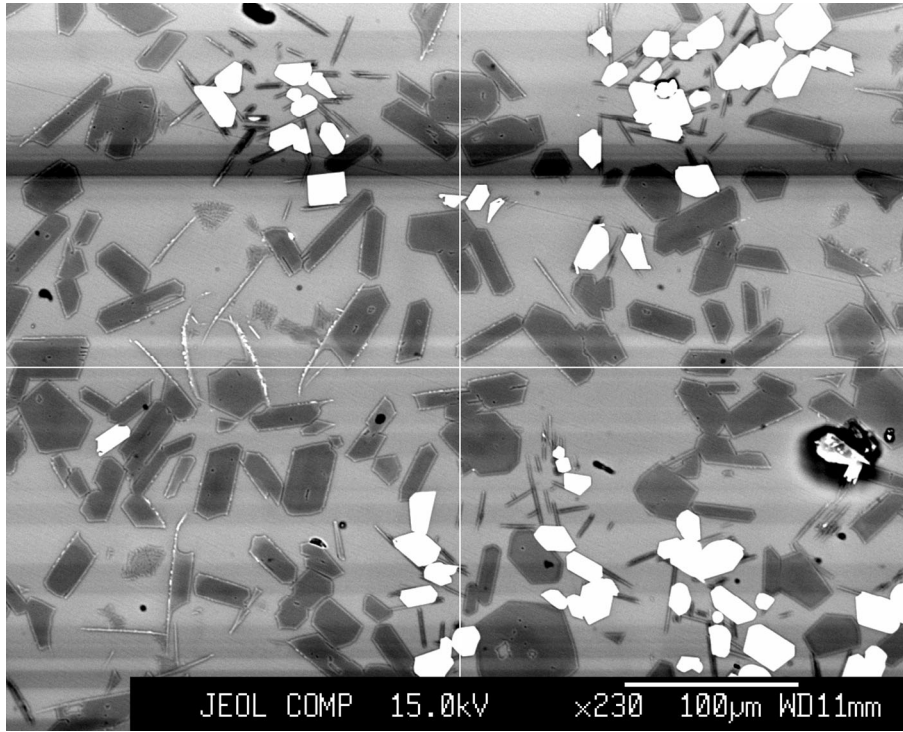


Fig. 4—Microphotograph of sample no. 3 showing the 3-phase equilibrium of the liquid (L), the solid  $V_2O_3$ - $Al_2O_3$  phase (VA), and the solid  $CaO$ - $Al_2O_3$ - $V_2O_3$  phase (CAV). The supercooled continuous liquid phase (L) is dark gray, the solid VA phase is light gray and the solid CAV phase is black.

Table III. Phases Found in the  $Al_2O_3$ - $CaO$ - $SiO_2$ - $V_2O_3$  System as well as the Composition and Relative Average Deviation of the Liquid Phase

Sample ID	Phases Present	Comp. Liquid Phase (Mass Pct)				Relative Deviation (Pct)			
		$Al_2O_3$	CaO	$SiO_2$	$V_2O_3$	$Al_2O_3$	CaO	$SiO_2$	$V_2O_3$
1	L	3.7	28.4	59.1	8.8	2.2	2.9	1.9	2.4
2	L, VA	8.7	27.1	56.0	8.1	1.7	2.0	0.8	3.3
3	L, VA, CAV	36.6	29.3	30.9	3.2	2.8	1.3	3.6	15.9
4	L, VA	10.6	30.1	50.1	9.2	0.4	0.2	0.1	1.0
5	L, VA	25.5	29.0	39.4	6.1	1.2	2.7	2.4	32.1
6	L, VA	20.3	29.1	43.6	7.1	0.5	0.3	0.2	1.9
7	L, VA	15.3	28.8	48.2	7.7	0.4	0.2	0.4	1.5
8	L, VA	10.1	29.0	52.3	8.5	0.5	1.0	0.5	5.3
9	L, VA	5.0	28.3	56.2	10.5	1.3	1.7	0.8	4.5
10	L, VA	35.4	31.7	31.1	1.8	3.6	4.9	2.9	
11	L, VA	27.7	33.8	37.1	1.4	0.4	0.5	0.5	
12	L, VA	17.4	33.1	46.8	2.7	0.8	0.5	0.6	3.2
13	L, VA	11.4	32.9	52.6	3.1	0.4	0.8	0.6	2.3
14	L, VA	5.6	32.7	58.4	3.2	1.1	0.9	0.4	2.4
15	L	20.5	30.7	47.1	1.8	0.5	0.3	0.3	
16	L	2.3	34.8	62.1	0.8	1.2	0.8	0.5	

The relative average deviation (RAD) of the EPMA analysis for compounds with more than 2 pct is also presented in Table III. RAD is defined by Eq. [1],

$$RAD(\text{pct}) = \frac{\left(\sum_{i=1}^N |x_i - \bar{x}|\right) / N}{\bar{x}} \times 100, \quad [1]$$

where  $x_1, \dots, x_N$  represent the data points,  $\bar{x}$  is the average value of the data, and  $N$  is the number of the total data points. The relative average deviation for the

data points was generally  $<2$  pct for  $Al_2O_3$ , CaO, and  $SiO_2$  and  $<6$  pct for  $V_2O_3$  in the liquid. The composition of the solid phases are listed in Table IV.

## IV. DISCUSSION

### A. Experimentally Determined Liquidus Surface

The compositions of the samples were aimed at 30 and 35 pct CaO, respectively. However, for various

experimental reasons, the CaO contents deviated somewhat from these targeted values. While the exact experimentally determined compositions are listed in Table III, to present the liquidus surface in a graphical manner, normalization is needed. The normalization was carried out according to the following procedure; *viz.* the CaO content within a range of 27.5 to 32.5 pct CaO was adjusted to 30 pct, while the concentrations of the remaining components were normalized in proportion to their original fractions with their sum being 70 pct. The CaO content within a range of 32.5 to 37.5 pct CaO was adjusted to 35 pct and the sum of the remaining components to 65 pct. Note that the readers should use the data listed in Table III for any thermodynamic calculation.

Figures 5 and 6 present the experimentally determined liquidus surface at 1873 K (1600 °C) in the section of 30 and 35 pct CaO, respectively. The liquidus surface in the section of 25 pct CaO, determined experimentally in an earlier study,<sup>[1]</sup> is reproduced in Figure 7. Note that these relationships are valid at an oxygen potential of  $9.37 \times 10^{-11}$  bar. In these figures, the liquid phase is marked with the symbol “●”. The coexistence of the two phases L and VA is marked with the symbol “▲”. The coexistence of the three phases L, VA, and CAV is marked with the symbol “■”. The line represents the phase boundary of the liquid–solid mixture, *i.e.*, slags with a composition along the line are saturated with V, while V is completely dissolved in slags with compositions below this line. Along each side

Table IV. Composition of the Solid Phases Found in the  $\text{Al}_2\text{O}_3\text{-CaO-SiO}_2\text{-V}_2\text{O}_3$  System

Sample ID	Phase	Comp. Solid Phase (Mass Pct)			
		$\text{Al}_2\text{O}_3$	CaO	$\text{SiO}_2$	$\text{V}_2\text{O}_3$
2	VA	0.6	0.7	0.1	98.6
3	VA	16.7	0.4	0.0	82.9
3	CAV	74.6	8.2	0.5	16.7
4	VA	1.0	0.6	0.1	98.3
5	VA	4.7	0.5	0.1	94.7
6	VA	3.0	0.4	0.0	96.6
7	VA	1.7	0.3	0.0	97.9
8	VA	0.8	0.4	0.0	98.8
9	VA	0.3	0.6	0.0	99.0
10	VA	8.1	0.3	0.1	91.5
11	VA	4.8	0.3	0.1	94.8
12	VA	1.9	0.2	0.1	97.8
13	VA	1.0	0.3	0.1	98.6
14	VA	0.4	0.3	0.1	99.2

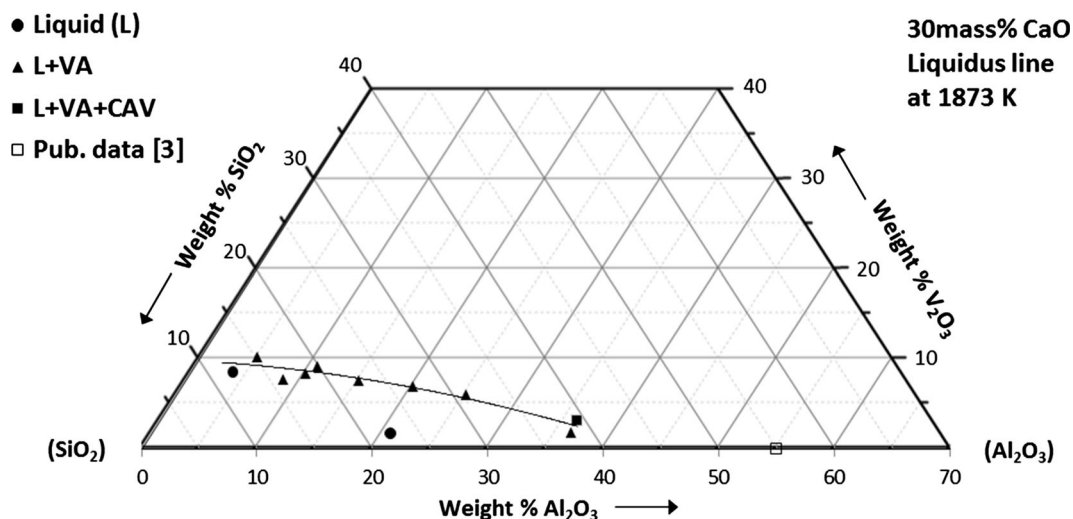


Fig. 5—Graphical presentation of the liquidus composition projected on the section of 30 pct CaO in the quaternary  $\text{Al}_2\text{O}_3\text{-CaO-SiO}_2\text{-V}_2\text{O}_3$  system at  $9.37 \times 10^{-11}$  bar and 1873 K (1600 °C). The liquid phase is marked with the symbol “●”. The coexistence of the two phases L and VA is marked with the symbol “▲”. The coexistence of the three phases L, VA, and CAV is marked with the symbol “■”. The liquidus surface for the 30 pct CaO section in the  $\text{Al}_2\text{O}_3\text{-CaO-SiO}_2$  system at 1873 K (1600 °C) is marked with the symbol “□”.

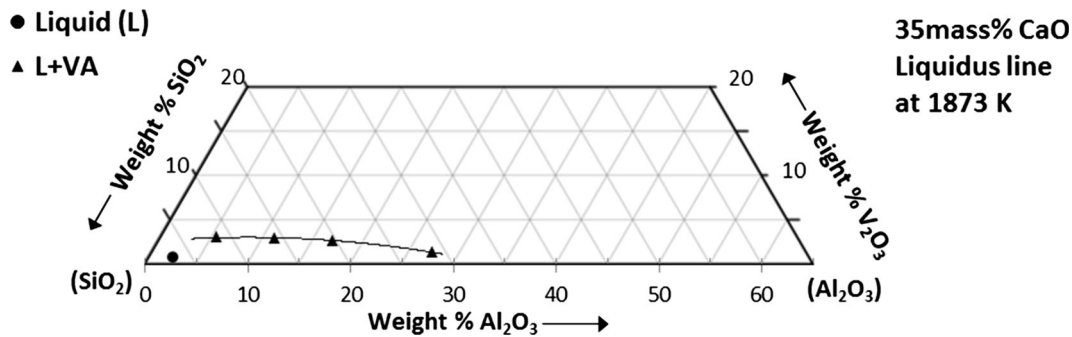


Fig. 6—Graphical presentation of the liquidus composition projected on the section of 35 pct CaO in the quaternary  $\text{Al}_2\text{O}_3\text{-CaO-SiO}_2\text{-V}_2\text{O}_3$  system at  $9.37 \times 10^{-11}$  bar and 1873 K (1600 °C). The liquid phase is marked with the symbol “●”. The coexistence of the two phases L and VA is marked with the symbol “▲”.

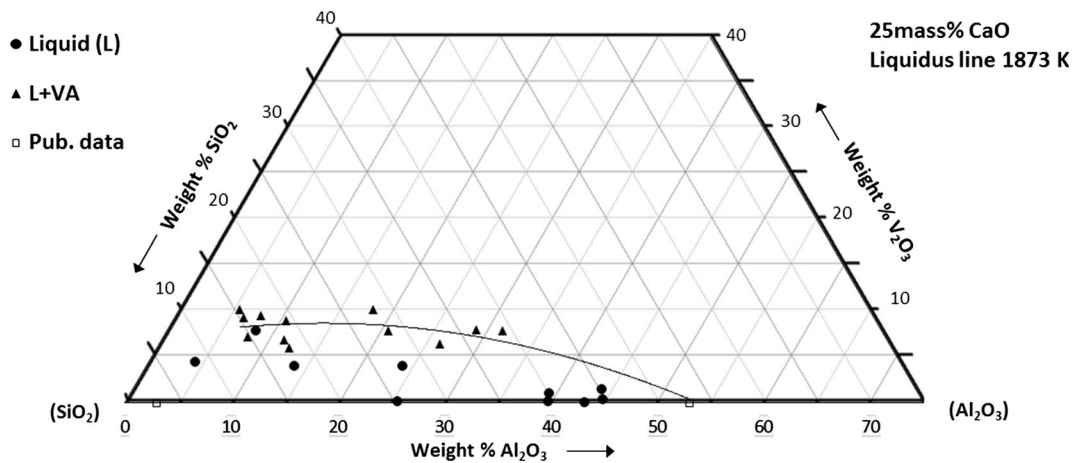


Fig. 7—Graphical presentation of the liquidus composition projected on the section of 25 pct CaO in the quaternary  $\text{Al}_2\text{O}_3\text{-CaO-SiO}_2\text{-V}_2\text{O}_3$  system at  $9.37 \times 10^{-11}$  bar and 1873 K (1600 °C). The liquid phase is marked with the symbol “●”. The coexistence of the two phases L and VA is marked with the symbol “▲”. The liquidus surface for the 25 pct CaO section in the  $\text{Al}_2\text{O}_3\text{-CaO-SiO}_2$  system at 1873 K (1600 °C) is marked with the symbol “□”.

of the triangles the three component systems are given by the 30 and 35 pct CaO sections of the  $\text{Al}_2\text{O}_3\text{-CaO-SiO}_2$ ,  $\text{Al}_2\text{O}_3\text{-CaO-V}_2\text{O}_3$ , and  $\text{CaO-SiO}_2\text{-V}_2\text{O}_3$  system. However, only data for the  $\text{Al}_2\text{O}_3\text{-CaO-SiO}_2$  system can be found in the literature.<sup>[3]</sup> The liquidus surface for the 30 pct section in the  $\text{Al}_2\text{O}_3\text{-CaO-SiO}_2$  system at 1873 K (1600 °C) is marked with the symbol “□”.

The solubility of V in the liquid phase decreases with increasing CaO content in the liquid. The V-solubility is especially low at both high CaO and  $\text{Al}_2\text{O}_3$  content in the liquid phase.

### B. Precipitation of Solid VA Phase

In a previous work investigating the  $\text{Al}_2\text{O}_3\text{-CaO(25 pct)-SiO}_2$  system,<sup>[1]</sup> the  $\text{Al}_2\text{O}_3$  solubility in  $\text{V}_2\text{O}_3$  was found to increase with increasing  $\text{Al}_2\text{O}_3$  content in the liquid as the  $\text{Al}_2\text{O}_3$  activity in the liquid increases with the increase of  $\text{Al}_2\text{O}_3$  in the liquid phase. In Figure 8, it is shown that the same correlation is also valid for the  $\text{Al}_2\text{O}_3\text{-CaO(30 pct)-SiO}_2$  and  $\text{Al}_2\text{O}_3\text{-CaO(35 pct)-SiO}_2$  system, *viz.* the  $\text{Al}_2\text{O}_3$  solubility in

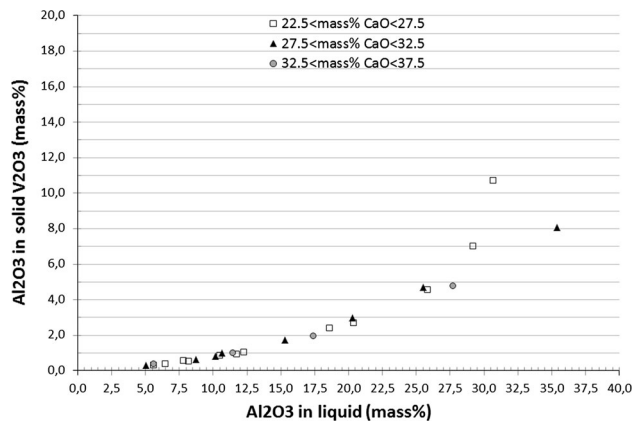


Fig. 8— $\text{Al}_2\text{O}_3$  in  $\text{V}_2\text{O}_3$  (VA phase) as a function of the  $\text{Al}_2\text{O}_3$  content in the liquid. Samples are grouped with respect to the CaO content in the liquid.

$\text{V}_2\text{O}_3$  increases with increasing  $\text{Al}_2\text{O}_3$  content in the liquid. In the figure, samples are grouped with respect to the CaO content in the liquid. The impact of the CaO

**Table V. The Results of the SEM–EDS Analyses of the Two Pellet Samples (Synthesized CAV Phase) as well as the WDS Analysis of the CAV Phase in Sample No. 3**

Sample ID	Comp. Solid Phase (Mass Pct)				Cations Per 19 Oxygens			
	Al <sub>2</sub> O <sub>3</sub>	CaO	SiO <sub>2</sub>	V <sub>2</sub> O <sub>3</sub>	Al	Ca	Si	V
3	74.6	8.2	0.5	16.7	10.3	1.0	0.1	1.6
Pellets 1	72.3	9.5	0.5	17.7	10.1	1.2	0.1	1.7
Pellets 2	70.9	9.5	1.4	18.2	9.9	1.2	0.2	1.7

content in the liquid on the solubility of Al<sub>2</sub>O<sub>3</sub> in the V<sub>2</sub>O<sub>3</sub> phase is small, especially when the Al<sub>2</sub>O<sub>3</sub> content in the liquid is <30 pct. Note that it is difficult to investigate the correlation above 30 pct Al<sub>2</sub>O<sub>3</sub> in the liquid at higher CaO contents as the V-solubility in the liquid is very low.

### C. Precipitation of Solid CAV Phase

The 3-phase equilibrium of L, solid VA phase, and a solid CAV phase was found in the Al<sub>2</sub>O<sub>3</sub>-CaO(30 pct)-SiO<sub>2</sub> system (sample no. 3) at high Al<sub>2</sub>O<sub>3</sub> content in the liquid. The components in the CAV phase were Al<sub>2</sub>O<sub>3</sub> (74.6 pct), CaO (8.2 pct), SiO<sub>2</sub> (0.5 pct), and V<sub>2</sub>O<sub>3</sub> (16.7 pct). In order to confirm the finding, this compound was also studied separately by synthesis. The starting materials used to prepare this compound have earlier been presented in Table I. The preparative technique involved careful grinding of equivalent quantities of the component oxides in an agate mortar and sintering pressed pellets. Two pellets with identical weight in composition were sintered in Pt-crucibles using the same experimental setup and procedure earlier described, *i.e.*, sintering at 1873 K (1600 °C) and at oxygen partial pressure of  $9.37 \times 10^{-11}$  bar for a duration of 48 hours. A sample of each pellets were mounted into conductive resin with carbon deposited in vacuum on the surface and analyzed with SEM–EDS analysis (Zeiss Merlin FE-SEM with an Oxford EDS detector) at 20 kV and 1 nA. The remaining parts of the two pellets were ground using an agate mortar and then used for determination of the crystallographic parameters using a Panalytical Empyrian Diffractometer, equipped with a Pixcel 3D detector and Cu-K $\alpha$  radiation. The XRD pattern was recorded from 5 to 90 deg  $\sin 2\theta$  at 0.026 deg/step and 88 s/step.

The results of the SEM–EDS analysis for the two pellet samples as well as the composition of the solid CAV phase found in sample no. 3 using WDS analysis are presented in Table V. The WDS analysis of sample no. 3 reveals a stoichiometric relation that is identical to calcium hexaluminate (CaAl<sub>12</sub>O<sub>19</sub> or CaO·6Al<sub>2</sub>O<sub>3</sub>) which occurs in nature as the mineral hibonite. This compound is also reported to crystallize from liquid Al<sub>2</sub>O<sub>3</sub>-CaO-SiO<sub>2</sub> melts with high Al<sub>2</sub>O<sub>3</sub> contents.<sup>[3]</sup>

The mineral hibonite has magnetoplumbite-type structure with the general crystallochemical formula of A<sup>(12)</sup>M<sup>(6)</sup>M<sub>2</sub><sup>(5)</sup>M<sub>3</sub><sup>(4)</sup>M<sub>4</sub><sup>(6)</sup>M<sub>5</sub><sup>(6)</sup>O<sub>19</sub>. Calcium occurs in 12-fold coordination (site A), whereas Al<sup>3+</sup> ions are distributed over three distinct octahedral sites (M1, M4, and M5), one tetrahedral site (M3) and a trigonal

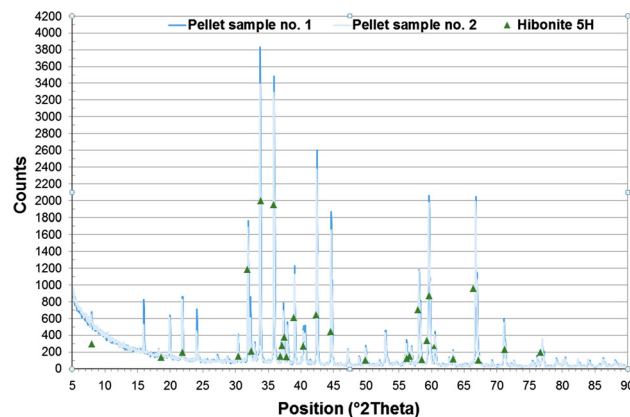


Fig. 9—Diffraction pattern of synthesized CAV phase.

bipyramidal site providing five-fold coordination by oxygen ions (M2). Hibonite has also the ability to accommodate a wide variety of ions, with different valence and coordination including V.<sup>[4]</sup> Despite this ability insignificant deviation from the stoichiometry: Ca = 1; (Al + V + Fe + Cr + Mg + Ti + Si + Sc) = 12 and O = 19 is usually reported.<sup>[5]</sup> Only a few references indicate that some meteoritic hibonites are highly nonstoichiometric.<sup>[6,7]</sup>

The diffraction patterns of the two pellet samples are shown in Figure 9. As shown in the figure, the crystal is identified as the mineral hibonite 5H with the chemical formula CaO((AlFe)O<sub>3</sub>)<sub>6</sub>.<sup>[8]</sup> It can, therefore, be concluded that the CAV phase found in this study is in fact fractionation of V into hibonite.

One reason that the CAV phase was not found in sample 10, situated close to sample no. 3 in Figure 6, could be due to that the ratios of the mixed powders for the two samples are different. The weighed in composition of Al<sub>2</sub>O<sub>3</sub> in sample no. 3 (3-phase equilibrium of L, VA, and CAV) was 44.24 pct and in sample no. 10 (2-phase equilibrium of L and VA) 33.29 pct while at the same time the Al<sub>2</sub>O<sub>3</sub> content in the liquid was quite similar, 36.6 and 35.4 pct, respectively. This surplus of Al<sub>2</sub>O<sub>3</sub>, except for the Al<sub>2</sub>O<sub>3</sub> going into solid solution (VA phase), could be the driving force for forming the Al<sub>2</sub>O<sub>3</sub>-rich CAV phase.

## V. CONCLUSIONS

The V-solubility in the Al<sub>2</sub>O<sub>3</sub>-CaO(30 mass pct)-SiO<sub>2</sub> and Al<sub>2</sub>O<sub>3</sub>-CaO(35 mass pct)-SiO<sub>2</sub> system at 1873 ± 4 K (1600 °C) and at a fixed oxygen potential ( $9.37 \times$



$10^{-11} \pm 3.8 \times 10^{-12}$  bar) was determined experimentally. EPMA analyses were made to identify the phases present and their compositions. The main findings could be summarized as:

1. The solubility of V-oxide increases with decreasing  $\text{Al}_2\text{O}_3$  and CaO content in the liquid.
2. The maximum V-solubility is up to 7 mass pct (given as V).
3. Samples saturated with V-oxide are either in a 2-phase region consisting of liquid (L) and a solid phase (VA), or in a 3-phase equilibrium of L, solid VA phase, and a solid  $\text{Al}_2\text{O}_3$ -rich phase (CAV).
4. The VA phase is a solid solution of  $\text{Al}_2\text{O}_3$  in V-oxide. The  $\text{Al}_2\text{O}_3$  solubility in this solid solution was found to increase with increasing  $\text{Al}_2\text{O}_3$  content in the liquid. As maximum, about 30 mass pct  $\text{Al}_2\text{O}_3$  was detected. The impact of the CaO content in the liquid on the solubility of  $\text{Al}_2\text{O}_3$  in  $\text{V}_2\text{O}_3$  was found to be small.
5. The CAV phase was identified as the mineral hibonite with fractionation of V (16.7 mass pct as  $\text{V}_2\text{O}_3$ ) into the crystal structure.

## ACKNOWLEDGMENTS

Funding and support from MISTRA, SSAB, LKAB, Ruukki, SSAB Merox, and Jernkontoret are gratefully acknowledged with special thanks to Dr. G. Ye and Dr. J. Björkvall of Swerea MEFOS. Thanks also to Stefan Andersson for technical support.

## REFERENCES

1. M. Lindvall, J. Gran, and D. Sichen: *CALPHAD*, 2014, vol. 47, pp. 50–55.
2. M. Lindvall, E. Rutqvist, G. Ye, J. Björkvall, and D. Sichen: *Steel Res. Int.*, 2010, vol. 81, pp. 105–11.
3. E.F. Osborn and A. Muan: *Phase Equilibrium Diagrams of Oxide Systems*, American Ceramic Society, Ohio, 1960, Plate 1.
4. R. Burns and V. Burns: *J. Geophys. Res.*, 1984, vol. 89, pp. C313–21.
5. J. Armstrong, G. Meeker, J. Huneke, and G. Wasserburg: *Geochim. Cosmochim. Acta*, 1982, vol. 46, pp. 575–95.
6. G. Macpherson, M.M. Bar-Matthews, T. Tanaka, E. Olsen, and L. Grossman: *Geochim. Cosmochim. Acta*, 1983, vol. 47, pp. 823–39.
7. A. Goresy and P. Ramdohr: *Meteoritics*, 1980, vol. 15, p. 286.
8. M. Harder and H. Mueller-Buschbaum: *Z. Naturforsch. B Anorg. Chem. Org. Chem.*, 1977, vol. 32, pp. 833–34.